Proton Capture Cross Sections at Low Energy

Matej Lipoglavšek

Jožef Stefan Institute, Ljubljana, Slovenia

Russbach, March 2013

Nuclear Reactions at Low Energies

Due to Coulomb repulsion the cross section σ for charged particle induced nuclear reactions drops rapidly with decreasing beam energy.

$$\sigma(E) = \frac{S(E)}{E} e^{-2\pi\eta},$$

where $\eta = Z_1 Z_2 e^2 / 4\pi\varepsilon_0 \hbar \sqrt{(2E/\mu)}$ is the Sommerfeld parameter. Exponential (Gamow) factor approximates barrier penetration probability.

$^{60}Ni(p, \gamma)^{61}Cu$ Cross Section

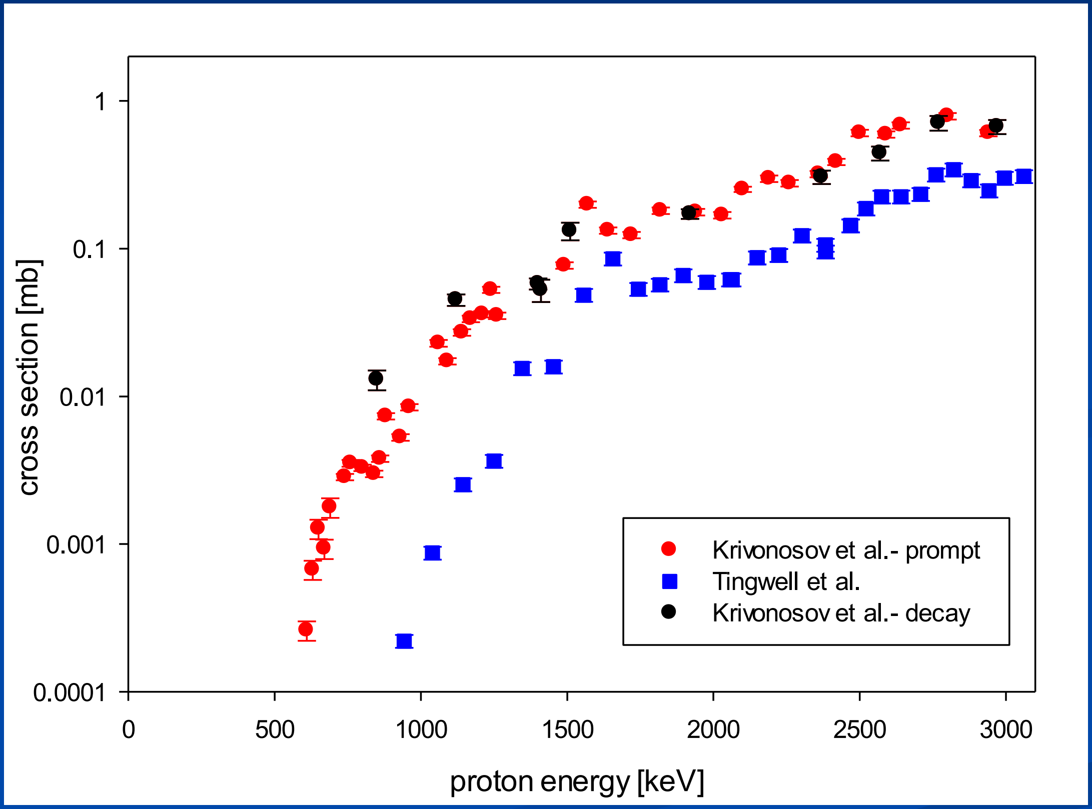

G. A. Krivonosov et al., Izv. Akad. Nauk SSSR **41** (1977) 2196.
C. I. W. Tingwell et al., Nucl. Phys. **A496** (1989) 127.

Electron Screening

Cross section increases at low energies when the interacting nuclei are not bare. Enhancement factor

$$f(E) = \frac{\sigma(E+U_e)}{\sigma(E)},$$

where U_e is the screeening potential.

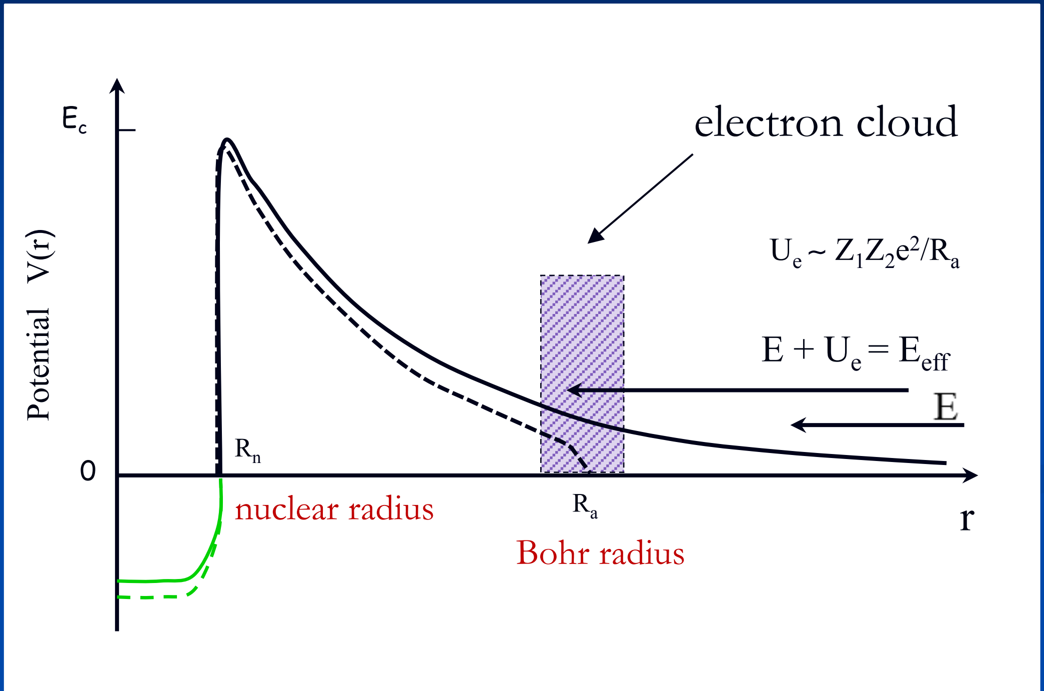

H. J. Assenbaum, K. Langanke and C. Rolfs, Z. Phys. A **327** (1987) 461. 246 citations (Web of Science).

$$\frac{R_n}{R_a} \approx 10^{-5} \Rightarrow U_e = \frac{e^2}{4\pi\varepsilon_0 R_a} = 27 \text{ eV for d+d reaction}$$

Previous Results 1

for d(d,p)t reaction from F. Raiola et al., Eur. Phys. J. A**19** (2004) 283.

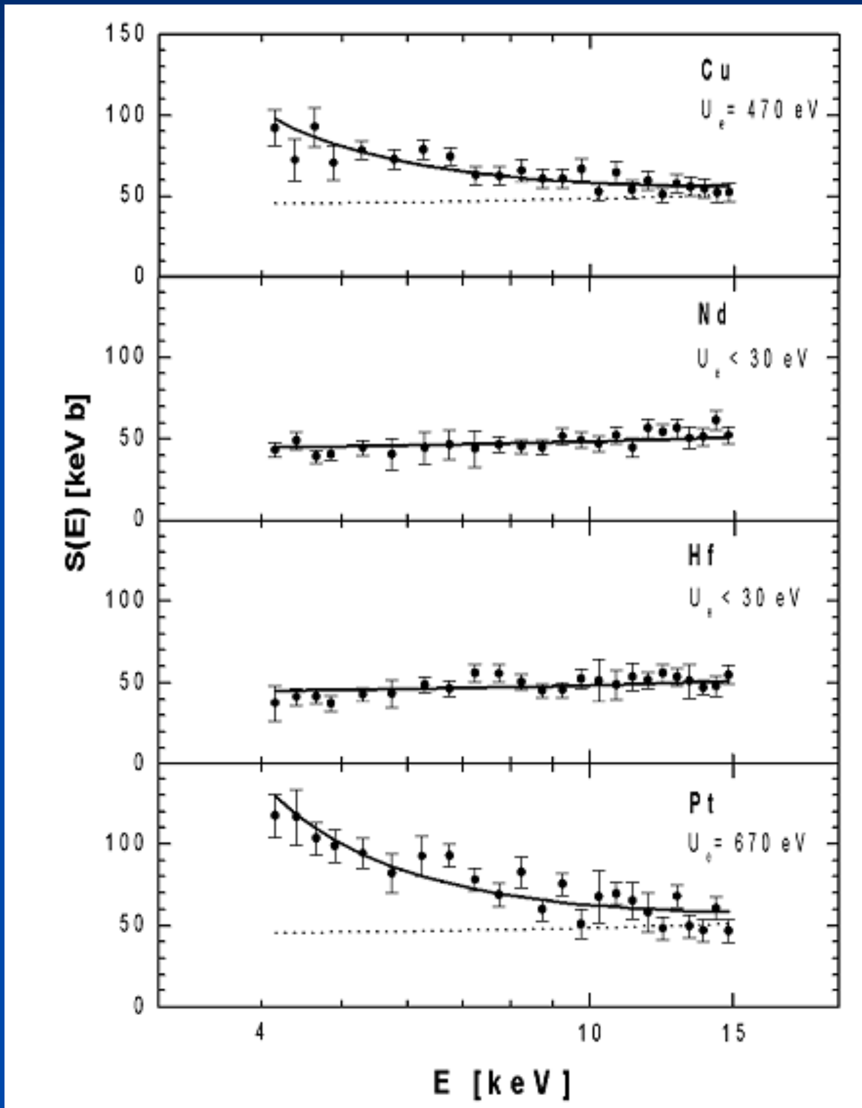

Material	U_e (eV)$^{(b)}$	Solubility $1/x$ $^{(c)}$	n_{eff} $^{(b)}$	n_{eff} (Hall)$^{(d)}$
		Metals		
Be	180±40	0.08	0.2±0.1	(0.21±0.04)
Mg	440±40	0.11	3.0±0.5	1.8±0.4
Al	520±50	0.26	3.0±0.6	3.1±0.6
V	480±60	0.04	2.1±0.5	(1.1±0.2)
Cr	320±70	0.15	0.8±0.4	(0.20±0.04)
Mn	390±50	0.12	1.2±0.3	(0.8±0.2)
Fe	460±60	0.06	1.7±0.4	(3.0±0.6)
Co	640±70	0.14	3.1±0.7	(1.7±0.3)
Ni	380±40	0.13	1.1±0.2	1.1±0.2
Cu	470±50	0.09	1.8±0.4	1.5±0.3
Zn	480±50	0.13	2.4±0.5	(1.5±0.3)
Sr	210±30	0.27	1.7±0.5	
Nb	470±60	0.13	2.7±0.7	(1.3±0.3)
Mo	420±50	0.12	1.9±0.5	(0.8±0.2)
Ru	215±30	0.18	0.4±0.1	(0.4±0.1)
Rh	230±40	0.09	0.5±0.2	(1.7±0.4)
Pd	800±90	0.03	6.3±1.3	1.1±0.2
Ag	330±40	0.14	1.3±0.3	1.2±0.3
Cd	360±40	0.18	1.9±0.4	(2.5±0.5)
In	520±50	0.02	4.8±0.9	
Sn	130±20	0.08	0.3±0.1	
Sb	720±70	0.13	11±2	
Ba	490±70	0.21	9.9±2.9	
Ta	270±30	0.13	0.9±0.2	(1.1±0.2)
W	250±30	0.29	0.7±0.2	(0.8±0.2)
Re	230±30	0.14	0.5±0.1	(0.3±0.1)
Ir	200±40	0.23	0.4±0.2	(2.2±0.5)
Pt	670±50	0.06	4.6±0.7	3.9±0.8
Au	280±50	0.18	0.9±0.3	1.5±0.3
Tl	550±90	0.01	5.8±1.2	(7.4±1.5)
Pb	480±50	0.04	4.3±0.9	
Bi	540±60	0.12	6.9±1.5	

Previous Results 2

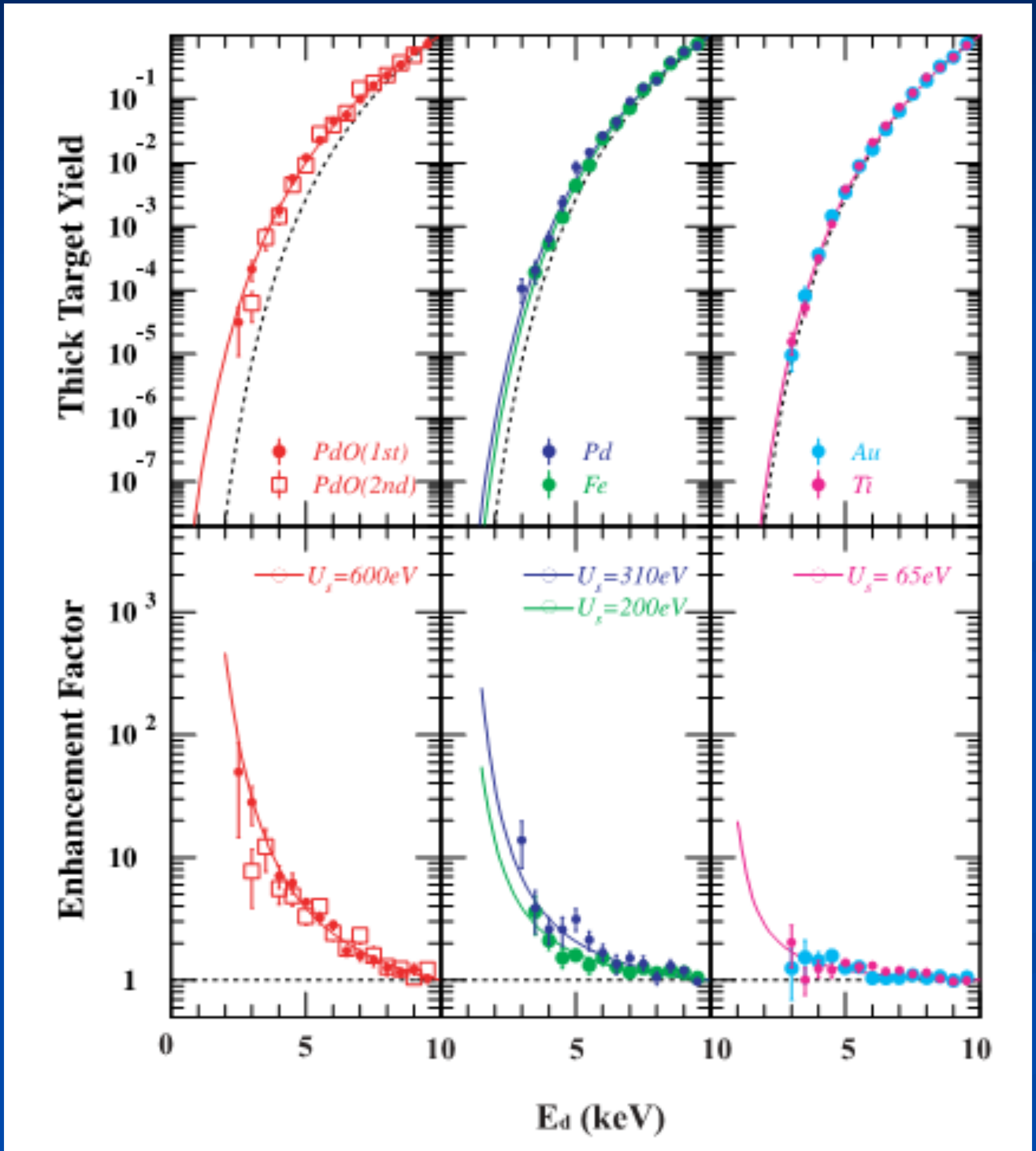

J. Kasagi, Prog. Theo. Phys. Suppl. 154 (2004) 365

for the d(d,p)t reaction
U_e=310±30 eV @ 7% H/Pd

=> concentration dependence

Previous Results 3

J. Cruz et al., Phys. Lett. B 624 (2005) 181.

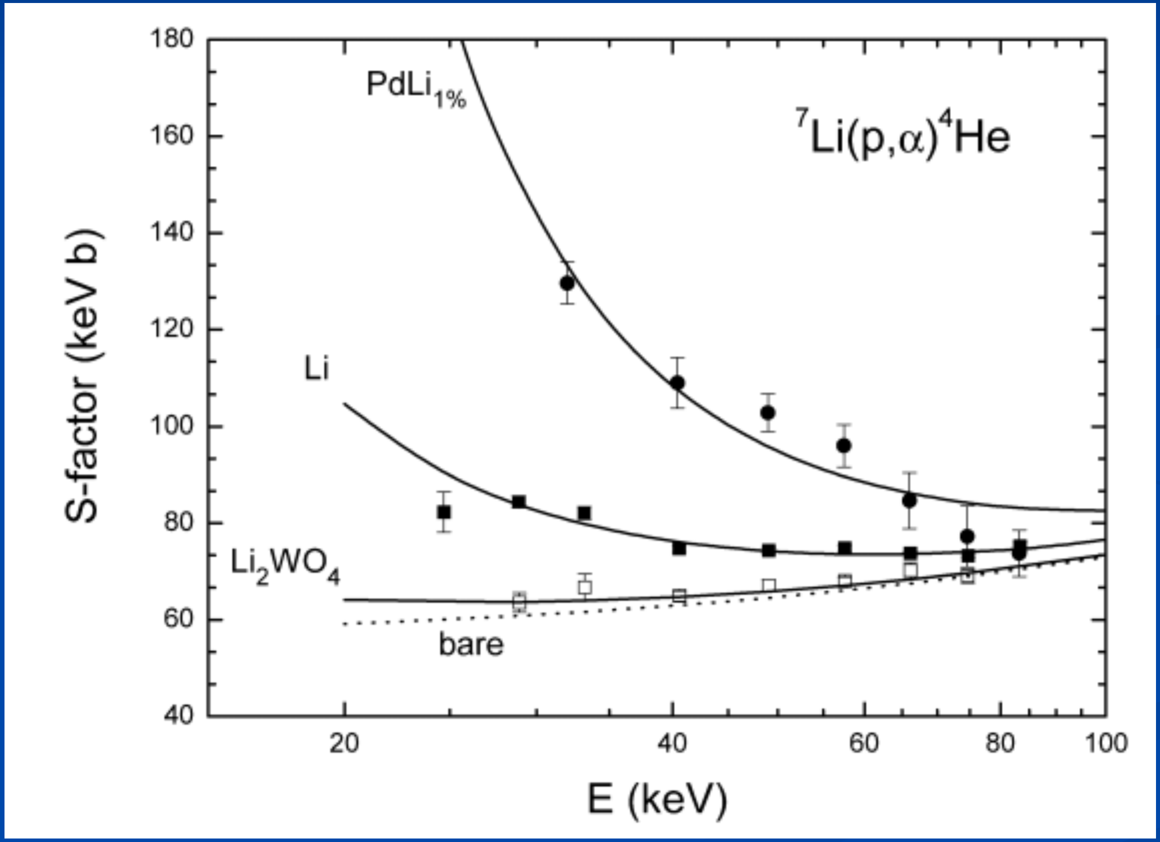

For $PdLi_{1\%}$:

$S(E)=0.055+0.21E-0.31E^2$ [MeV b]

$U_e=3.8$ keV

Previous Results 4

K. U. Kettner et al., J. Phys. G **32** (2006) 489.

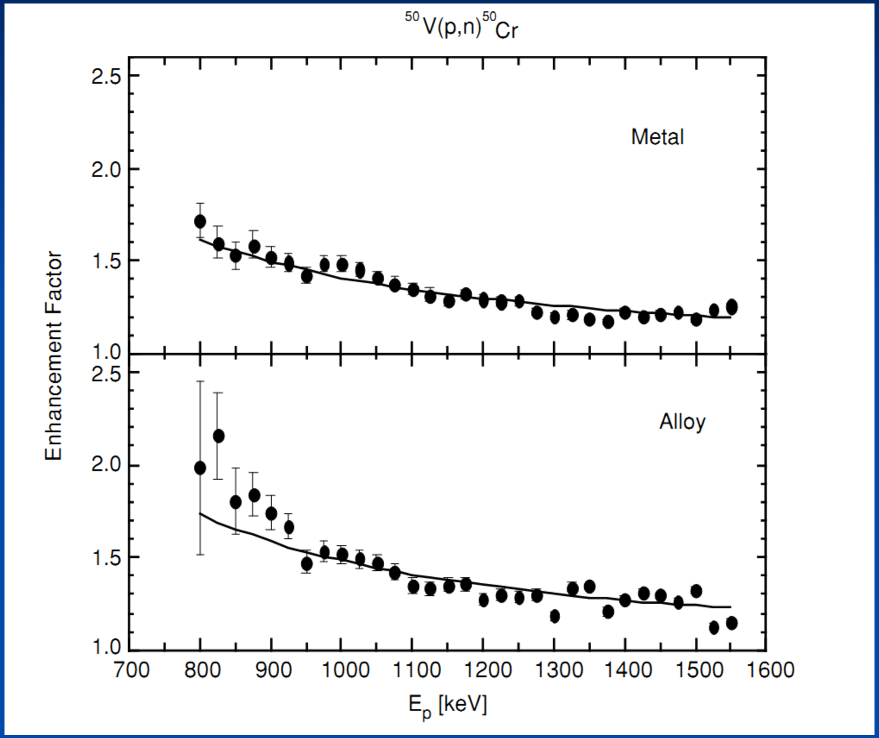

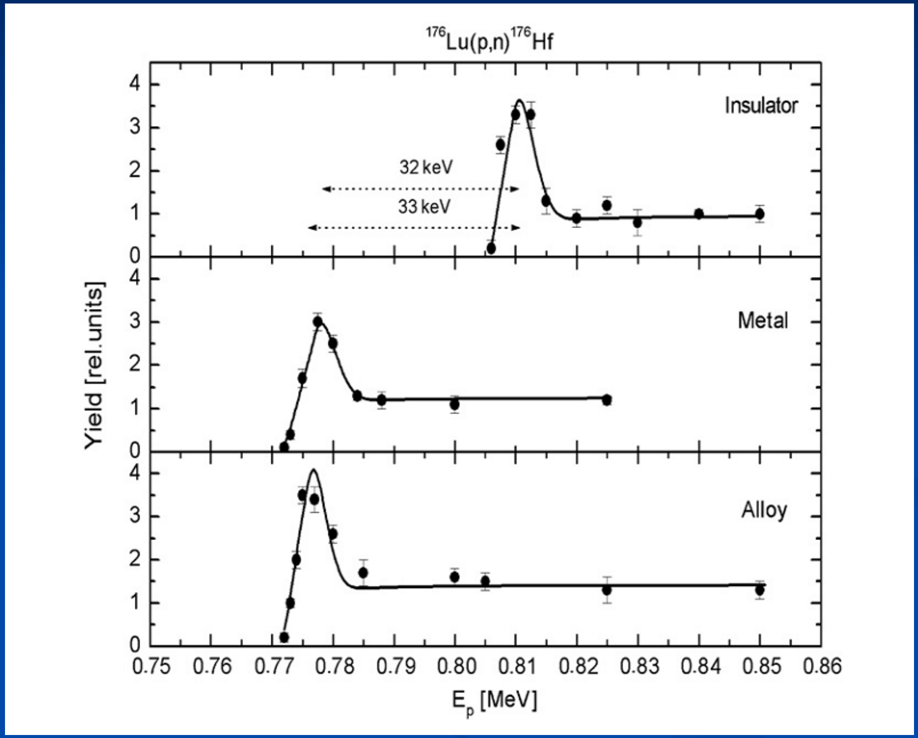

$^{50}V(p,n)^{50}Cr$ reaction in different environments: VO_2 insulator, V metal and $PdV_{10\%}$ alloy. Relative to the insulator, metal and alloy showed a large screening potential of $U_e = 27$ and 34 keV.

$^{176}Lu(p,n)^{176}Hf$ reaction in Lu_2O_3 insulator, Lu metal and $PdLu_{10\%}$ alloy; there is a narrow resonance and a shift in proton resonance energy of $U_e = 32$ and 33 keV for the metal and alloy, respectively, relative to the insulator.

$\Rightarrow U_e \propto Z$

Jožef Stefan Institute

300 km

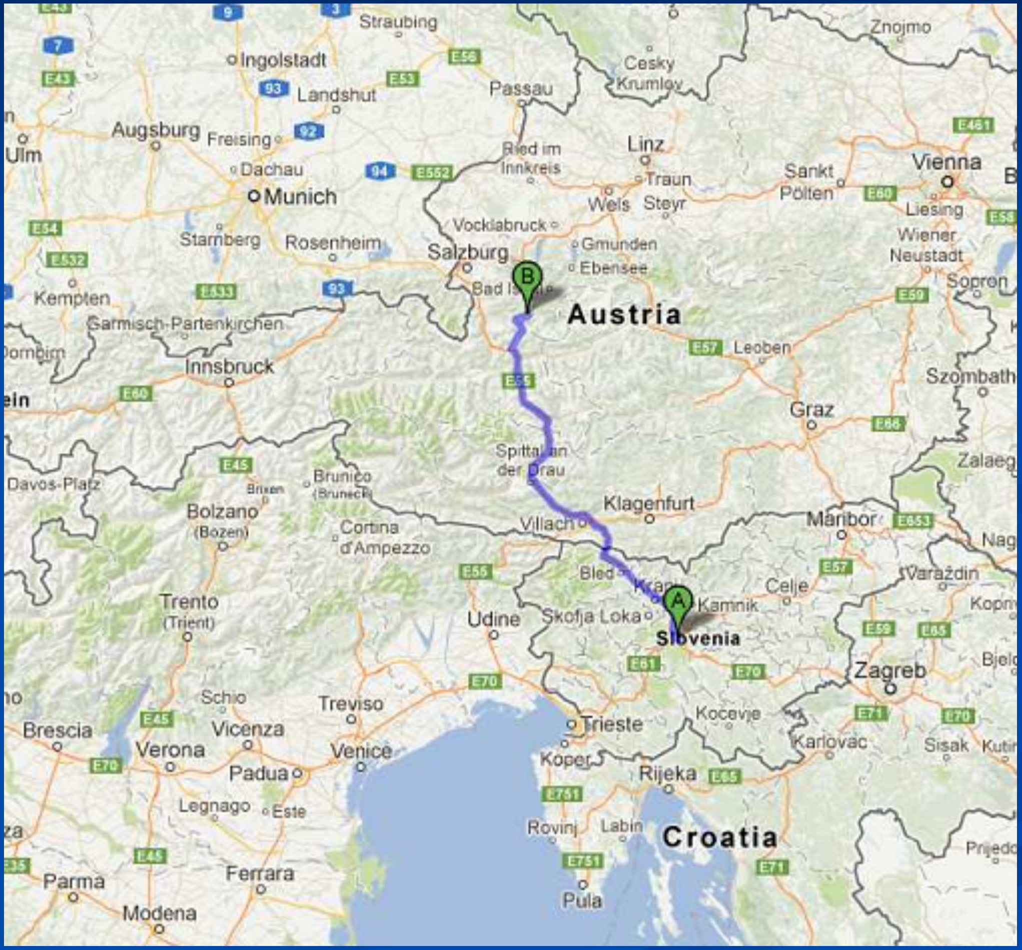

Measurements @ JSI

2 MV Tandem van de Graaf accelerator

Experimental setup:
2 X-ray detectors,
1 γ-ray detector,
charged particle detectors,
neutron detector.

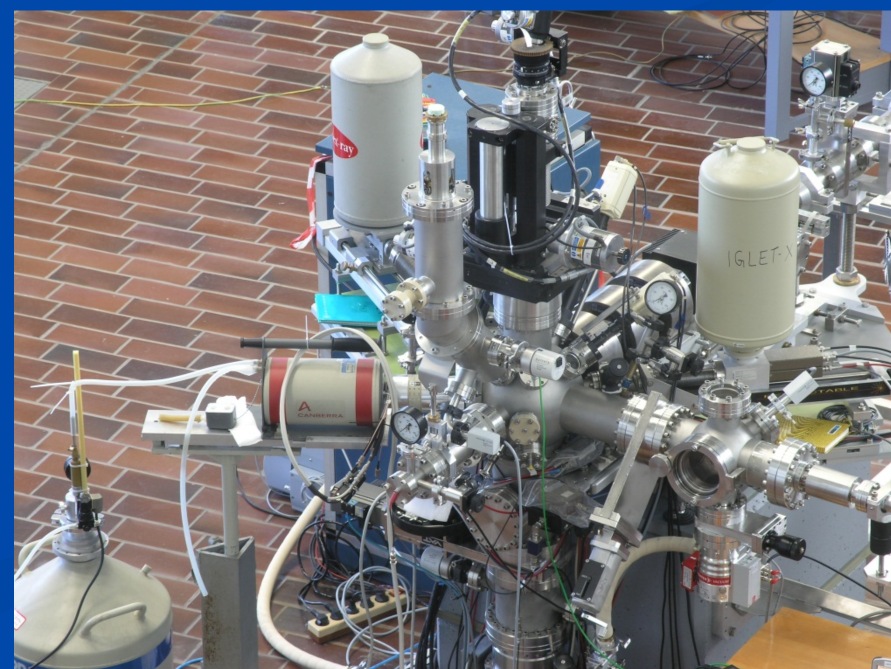

Electron screening in aluminum

(p,γ), (p,p´γ) and (p,nγ) reactions were studied on natural Ni and Al metals and NiO and Al_2O_3 insulators.

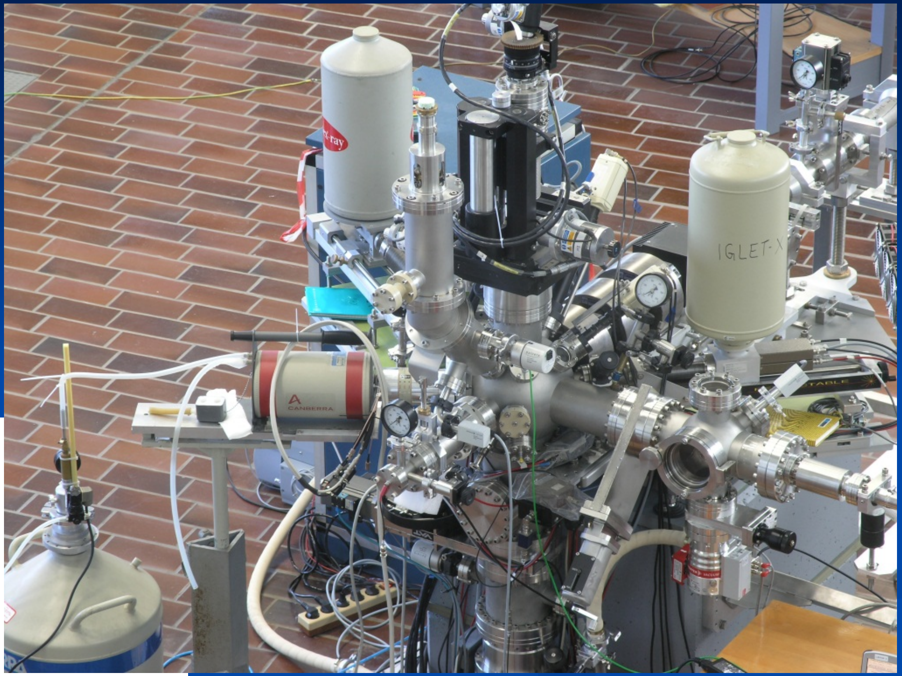

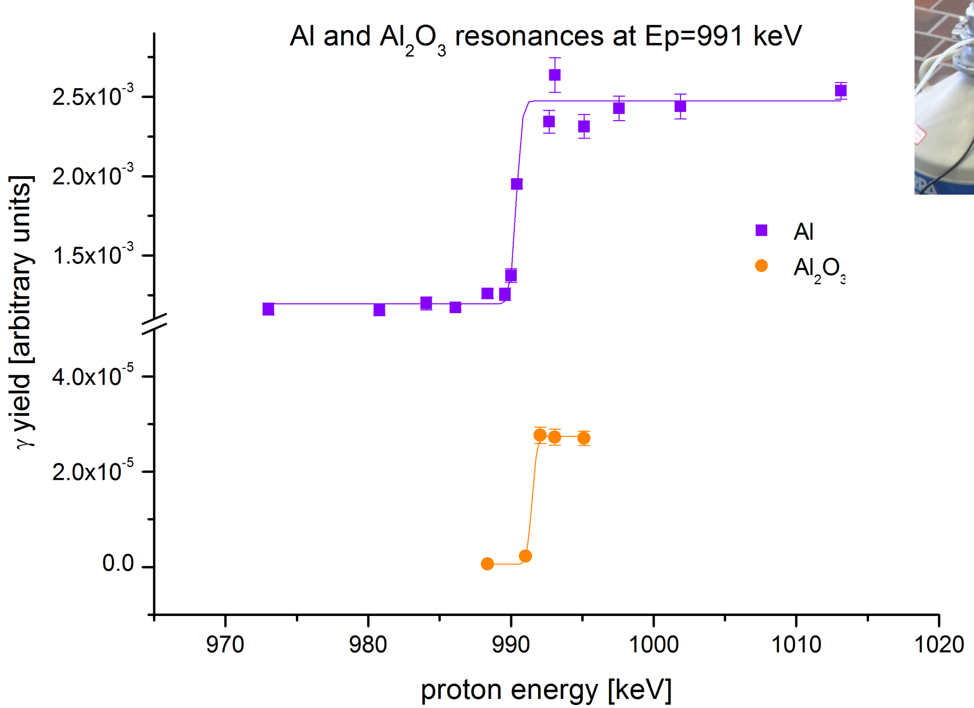

Characteristic γ rays were measured by a Ge detector: 1779 keV γ ray from $^{27}Al(p,\gamma)^{28}Si$ reaction

Nickel

3 γ rays from $^{58}Ni(p,\gamma)^{59}Cu$ reaction

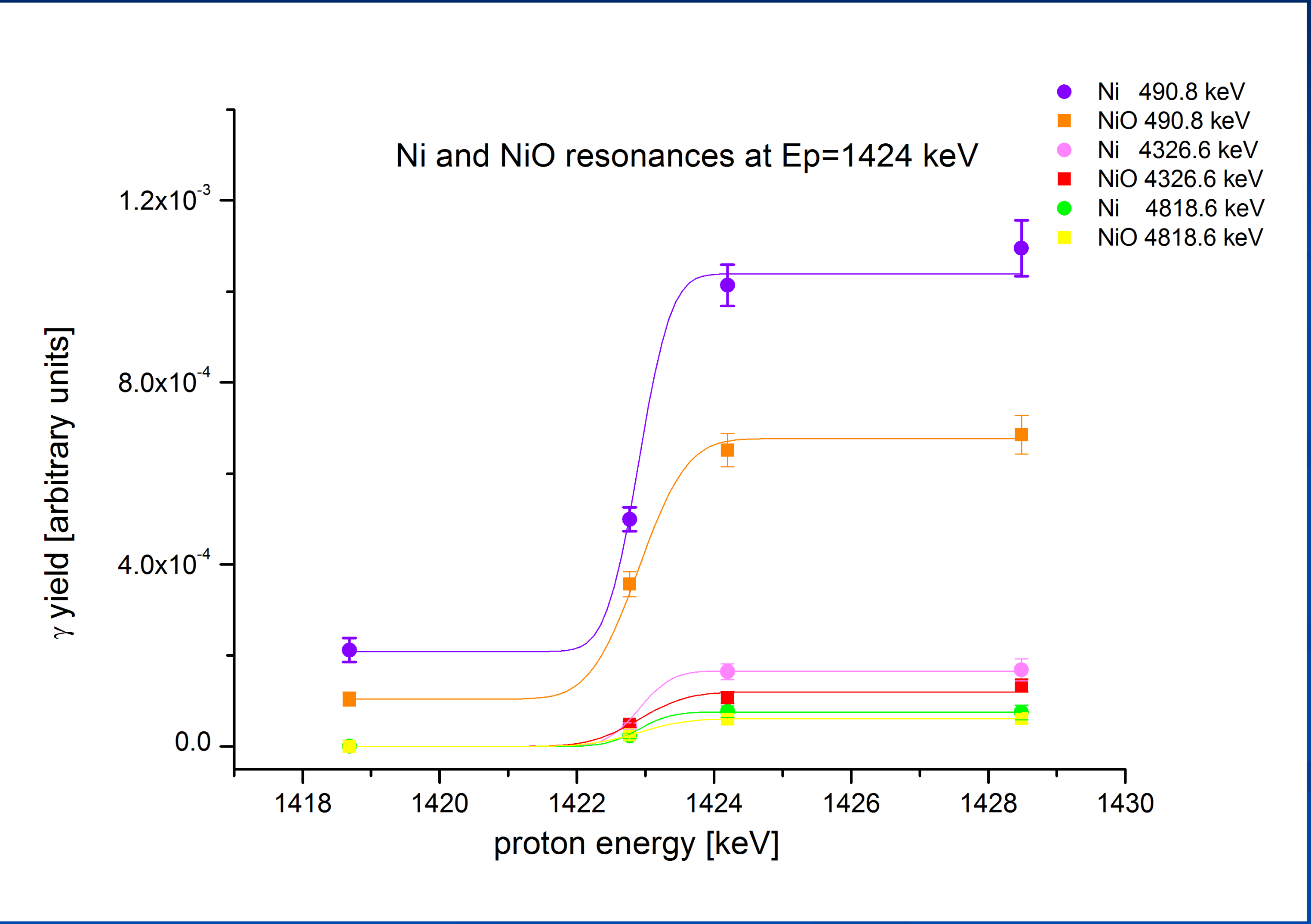

Nickel

1454 keV γ ray from $^{58}Ni(p,p'\gamma)^{58}Ni$ reaction

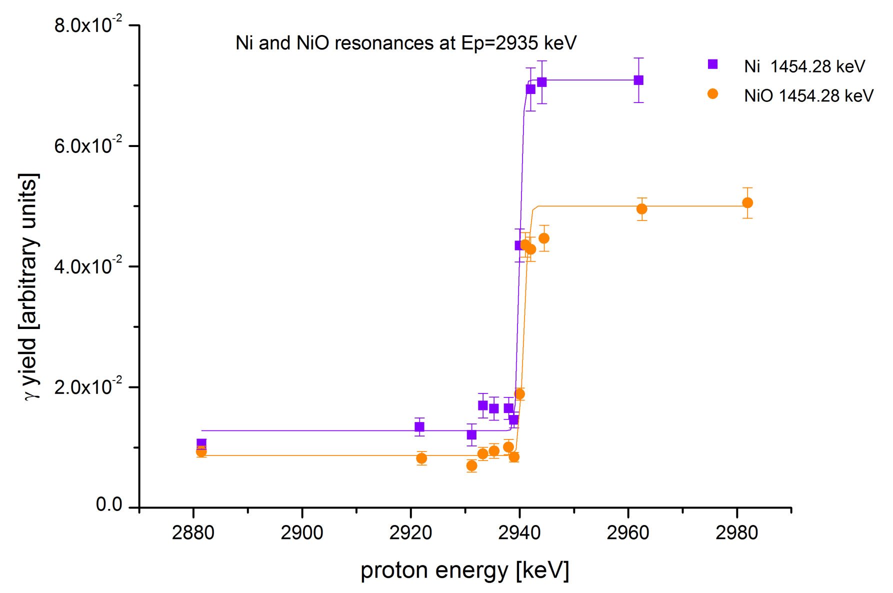

5231 keV γ ray from $^{58}Ni(p,\gamma)^{59}Cu$ reaction

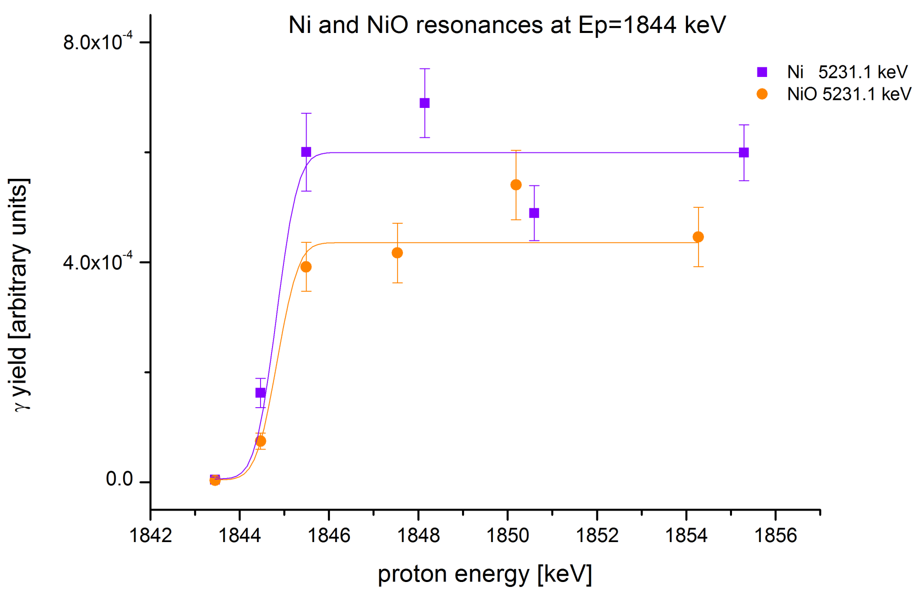

- No shift in resonance energy
- Difference in resonance strength

$^{58}Ni(p,\gamma)^{59}Cu$

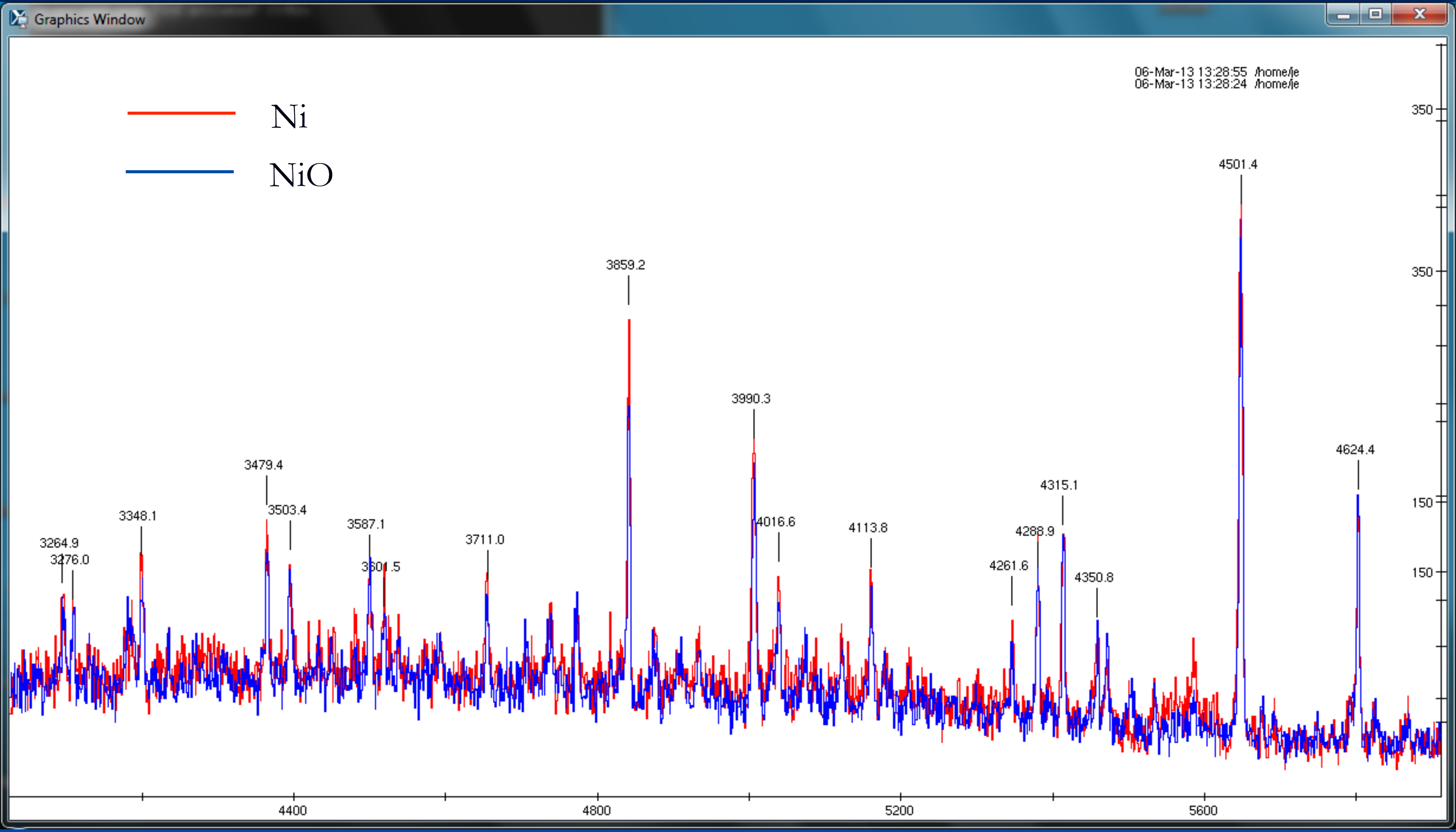

$^{60}Ni(p,\gamma)^{61}Cu$

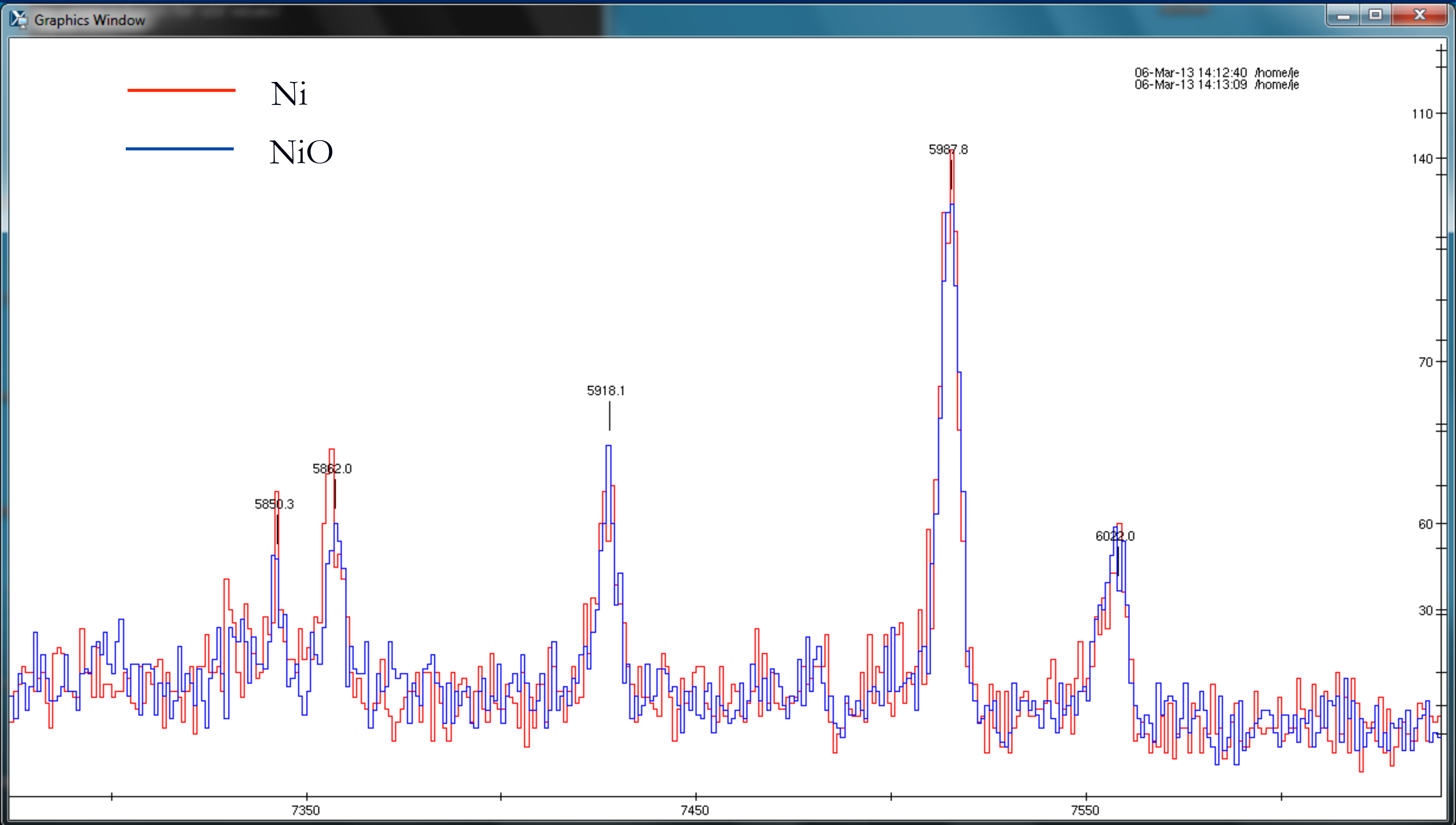

Enhancement factor

$$f(E) = \frac{\sigma(E+U_e)}{\sigma(E)}$$

$$f(E) = \alpha \frac{N_\gamma / N_p(Ni)}{N_\gamma / N_p(NiO)}$$

$$\alpha = \frac{M_{NiO} \frac{dE}{dx\rho}(NiO)}{M_{Ni} \frac{dE}{dx\rho}(Ni)}$$

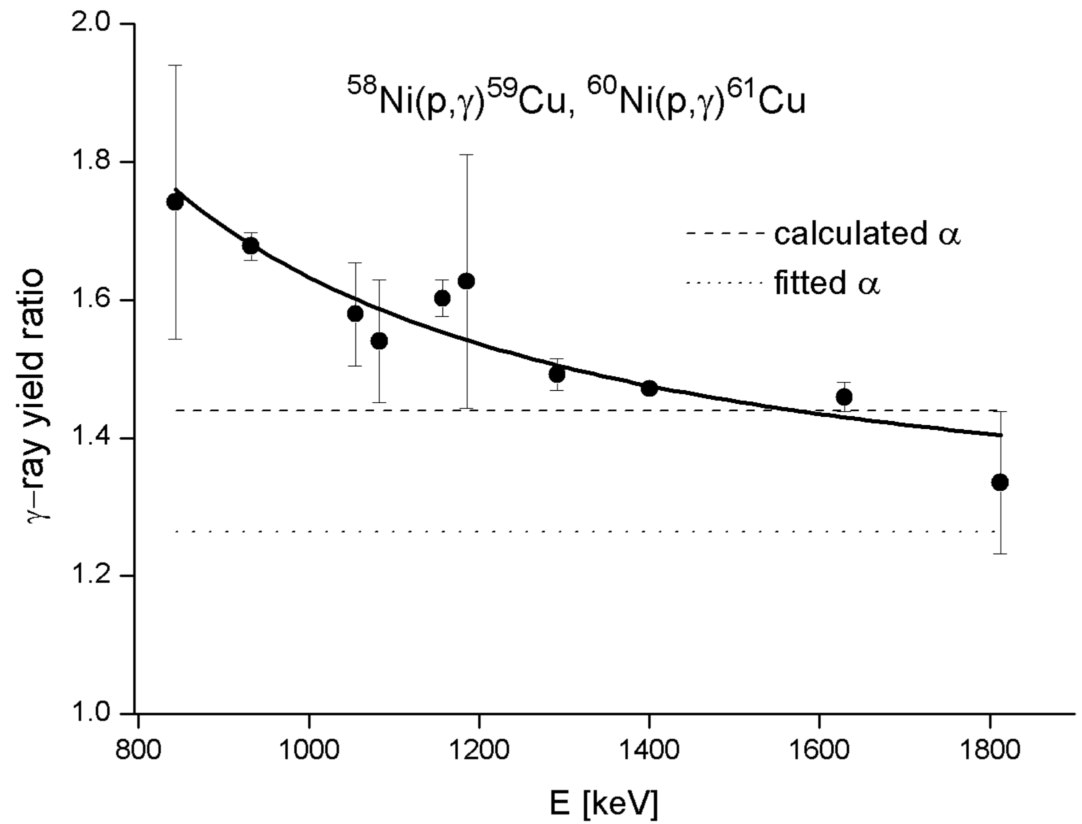

$$U_e = 19 \pm 4 \text{ keV}; \; \alpha = 1.26 \pm 0.02$$

^{64}Ni(p,n)^{64}Cu reaction

E γ =159 keV

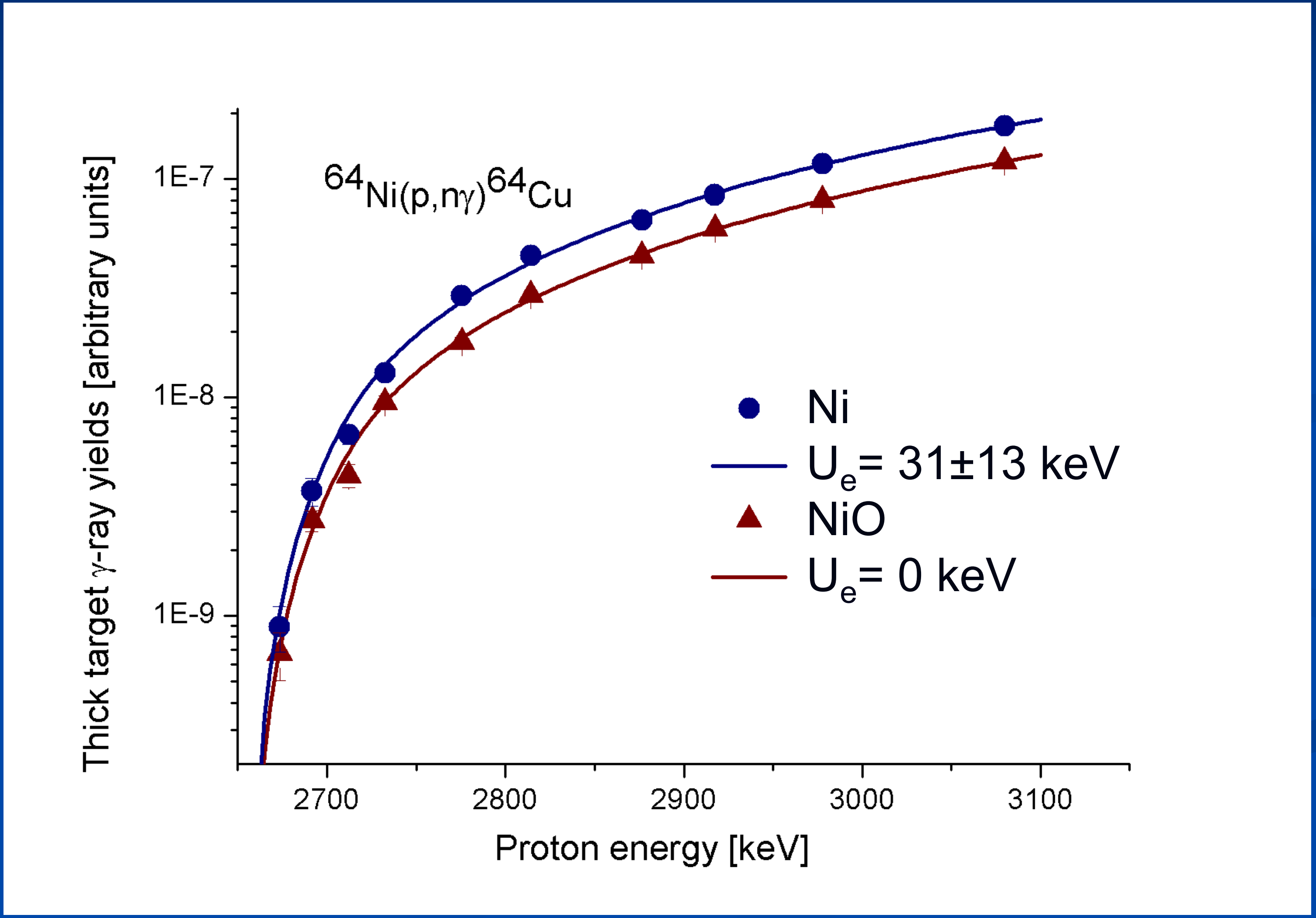

Electron screening calculation

Solving time dependent 3D Schrödinger equation on a lattice for the hydrogen electron in collision of neutral hydrogen and nickel atoms at hydrogen energy of 1.6 MeV.

t=0

t=collision

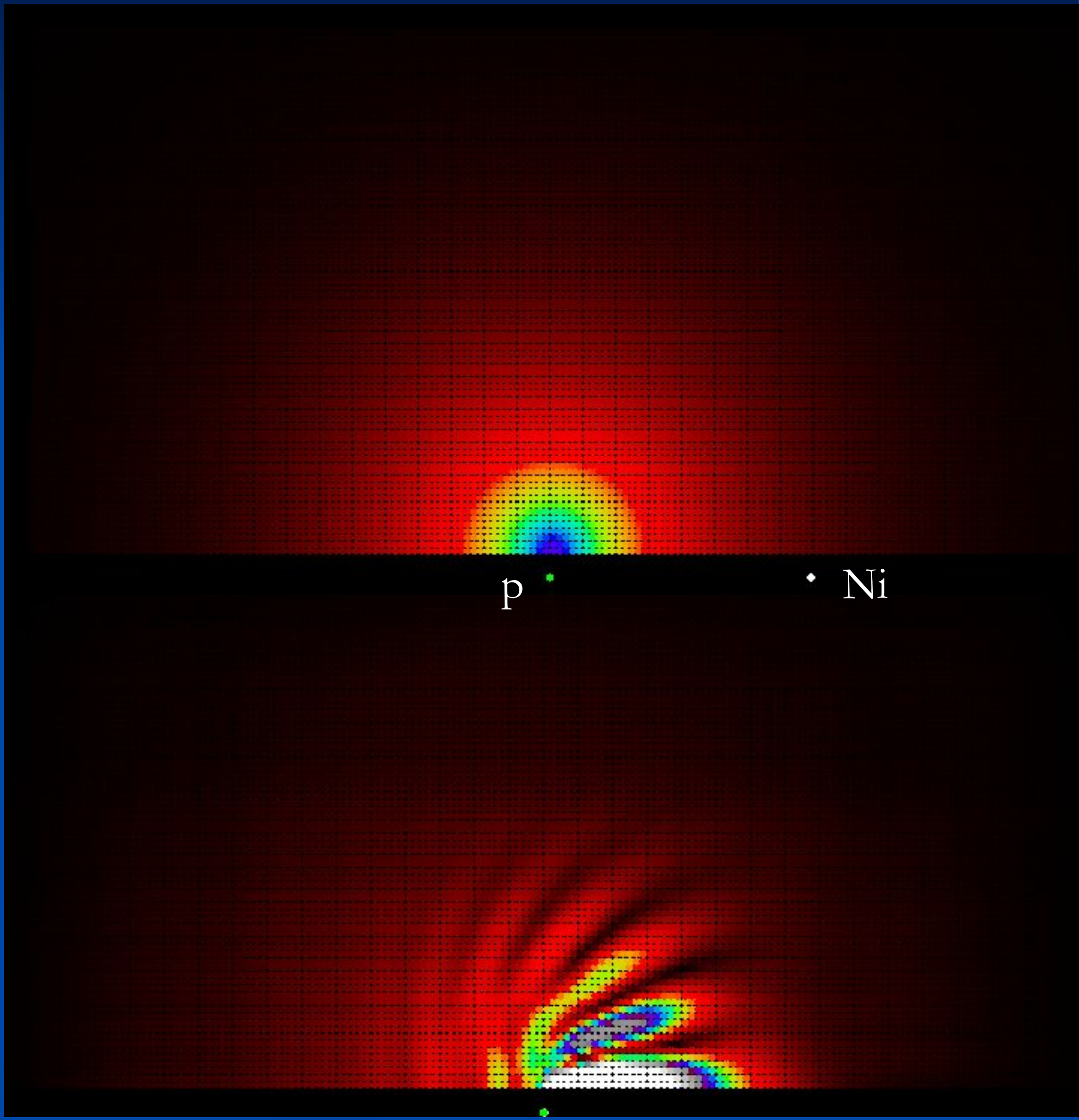

Electron density

Electron density at the place of the proton as a function of the distance between the proton and the nickel nucleus.

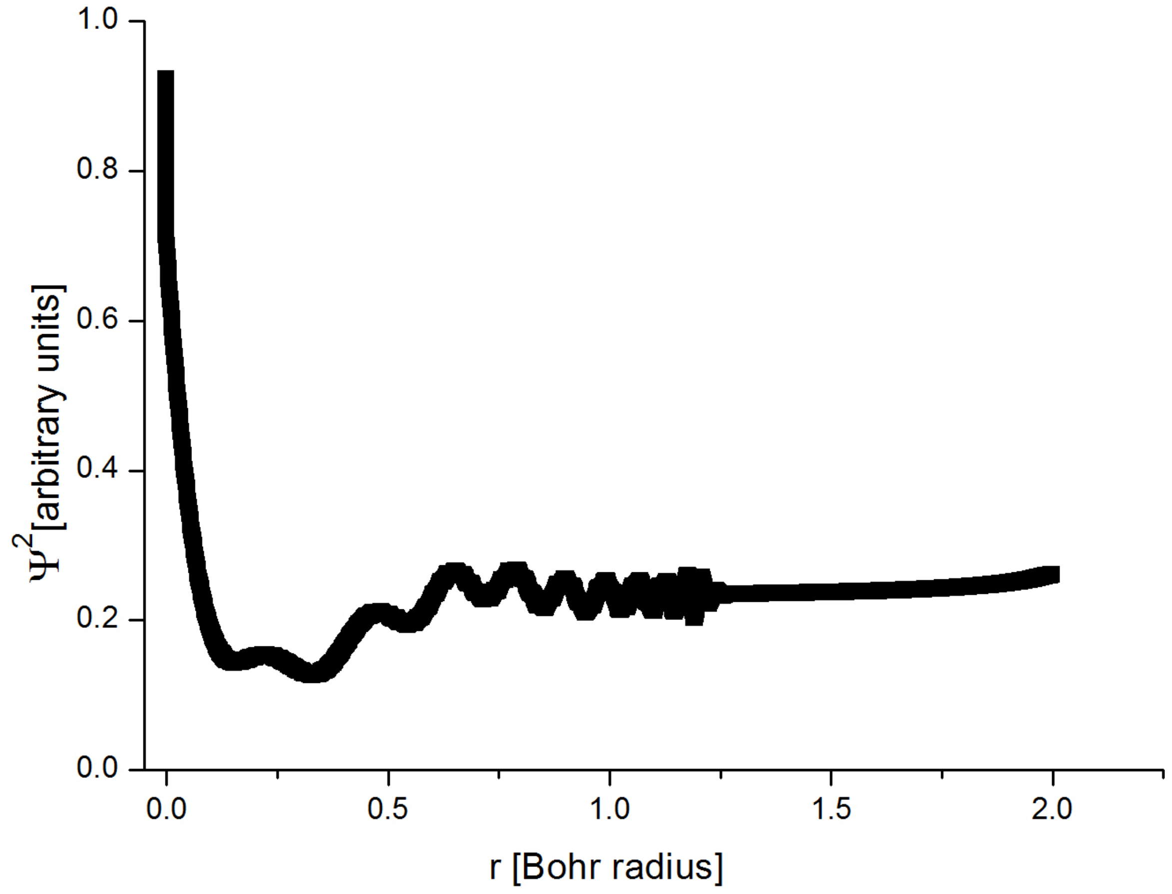

β^+/EC Decay of ^{61}Cu

^{61}Cu source	Half-life [h]
Ni metal	3.31(1)
NiO insulator	3.34(2)
Nucl. Data Sheets	3.333(5)

$N_x(Ni)/N_x(Ni$

$N_{511}(Ni)/N_{51}$

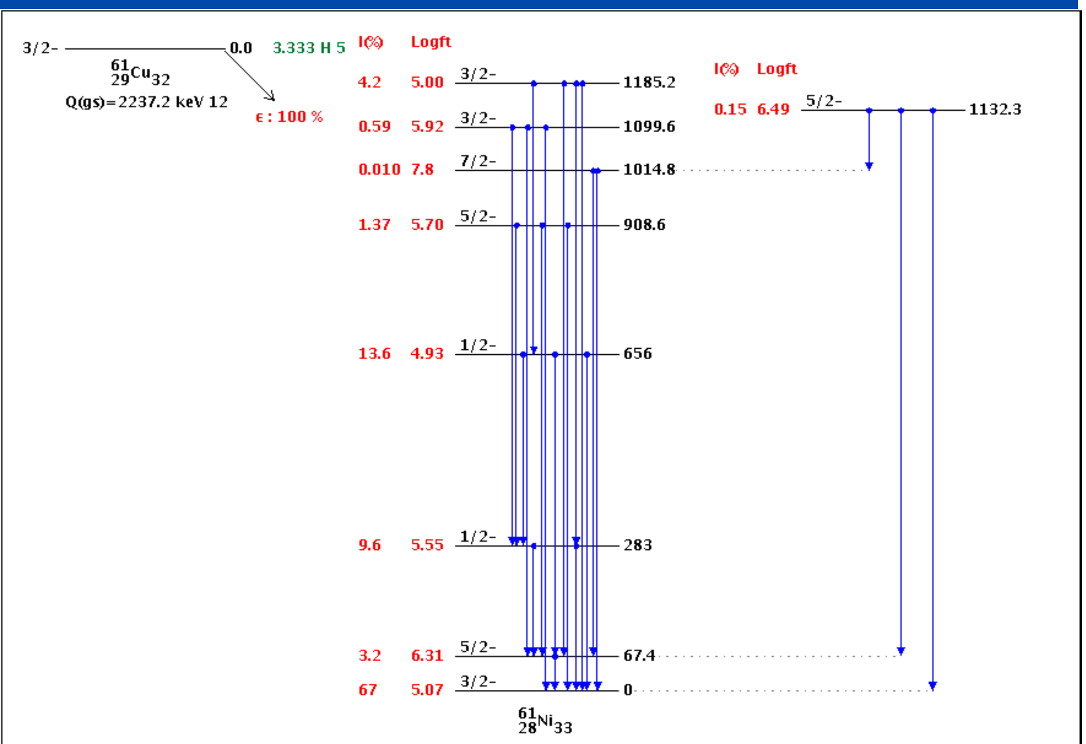

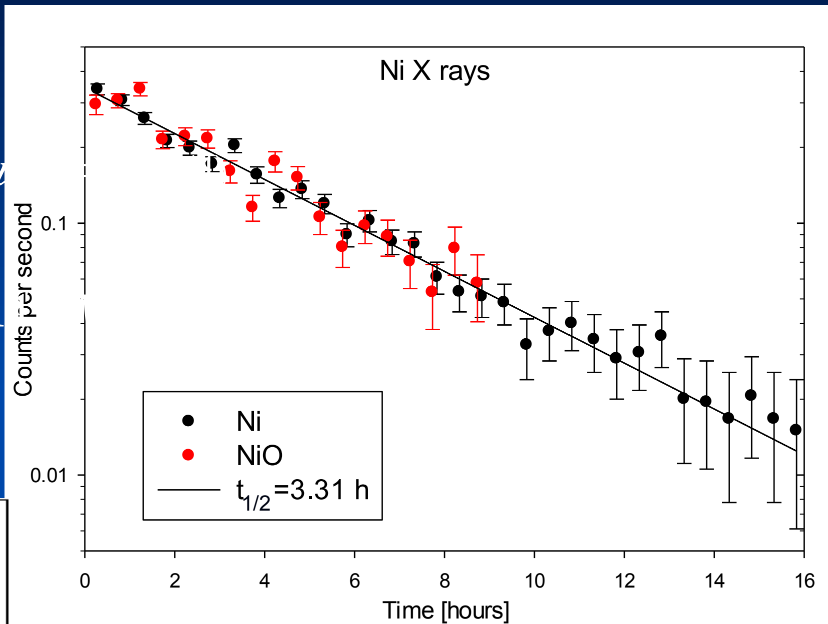

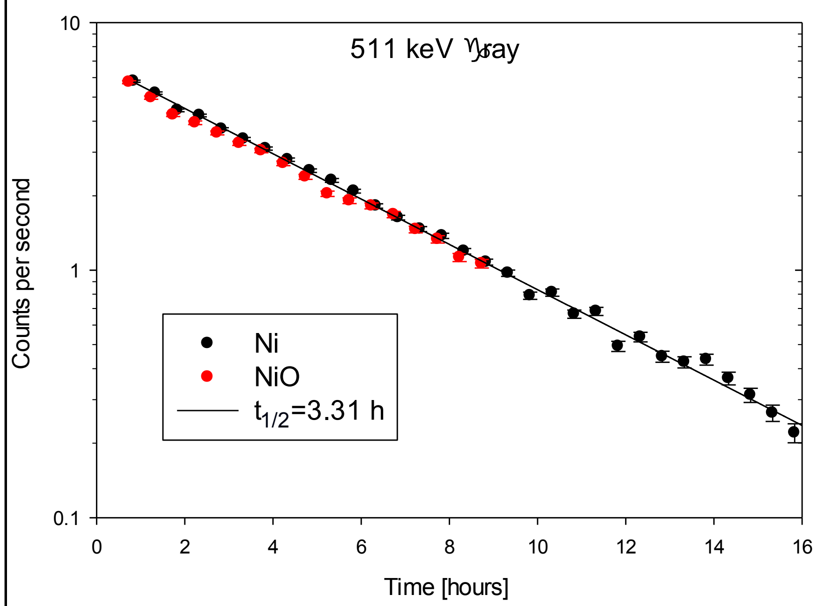

Conclusions

- All measured cross sections in metallic targets are not bare, but include electron screening. The same is true for resonance strengths.
- $U_e(Z=1;d,p)=200\text{-}800$ eV, $U_e(Z=3;p,\alpha)=3.8 \pm 0.5$ keV, $U_e(Z=23;p,n)=27 \pm 9$ keV, $U_e(Z=28;p,n)=31 \pm 13$ keV, $U_e(Z=28;p,\gamma)=19 \pm 4$ keV, $U_e(Z=72;p,n)=32 \pm 2$ keV.
- Electron screening is not a static but rather a dynamic effect, so the parameterization with a screening potential is questionable.
- Electron screening **IS** important in plasma.

Thanks to: Jelena Gajević, Toni Petrovič, Miha Škof, Andrej Likar, Žiga Šmit, Matjaž Vencelj, Primož Pelicon, Primož Vavpetič, Drago Brodnik, Aleksandra Cvetinović, Alberto Sanchez Ortiz

Thick Target Yields

α-particle yield calculation: $N_\alpha = 2N_{Li}\frac{\rho N_A}{M}\int_{E_0}^{0}\Omega W\frac{\sigma(E)}{dE_{Li}/dx}dE_{Li}$

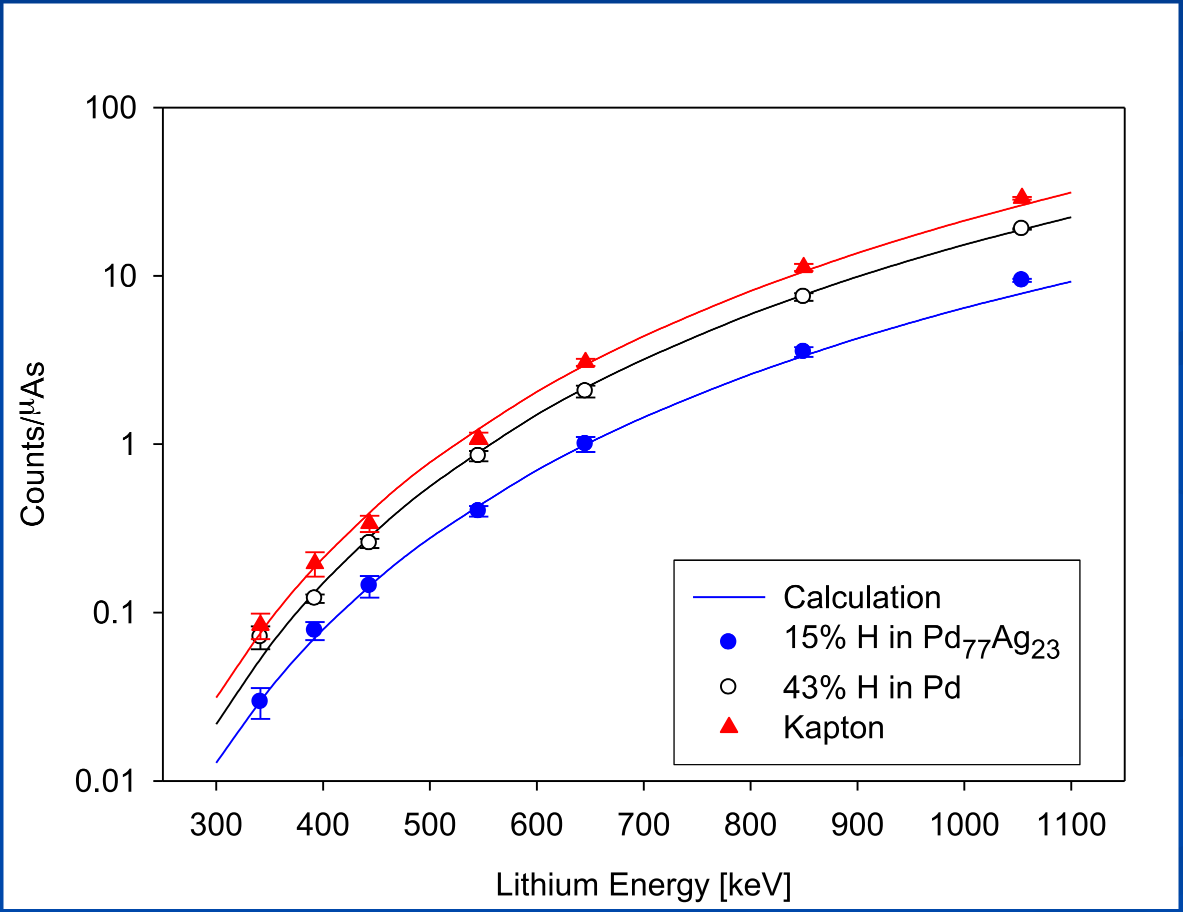

dE_{Li}/dx stopping power
Ω efficiency
W ang. distribution

Reaction: $^{1}H(^{7}Li,\alpha)^{4}He$

Electron density

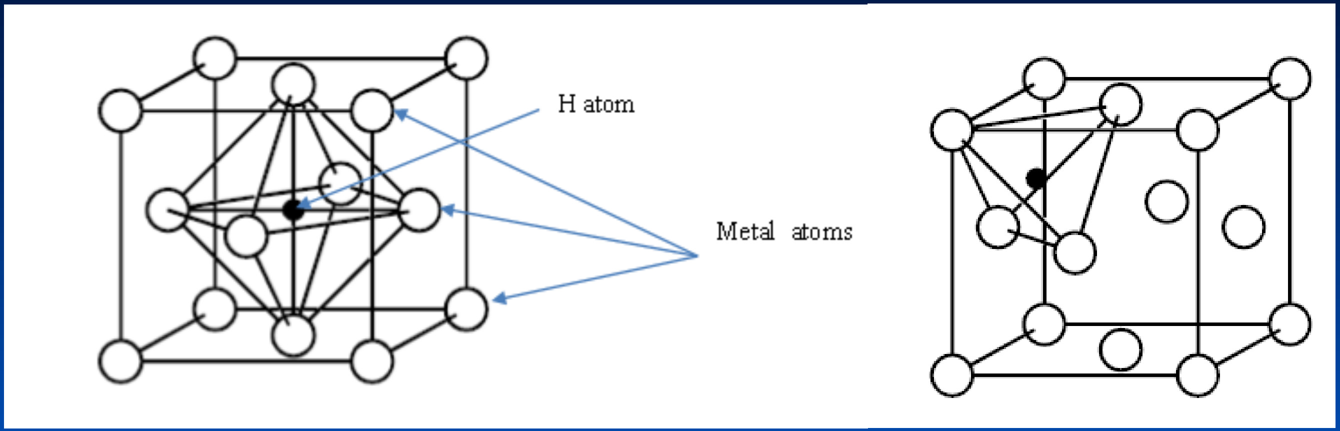

face centered cubic lattice

Octahedral position —stretching→ Tetrahedral position

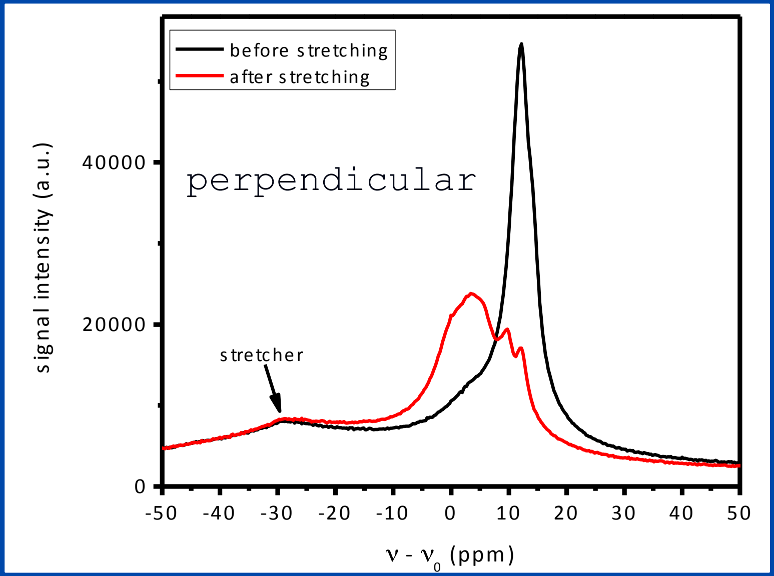

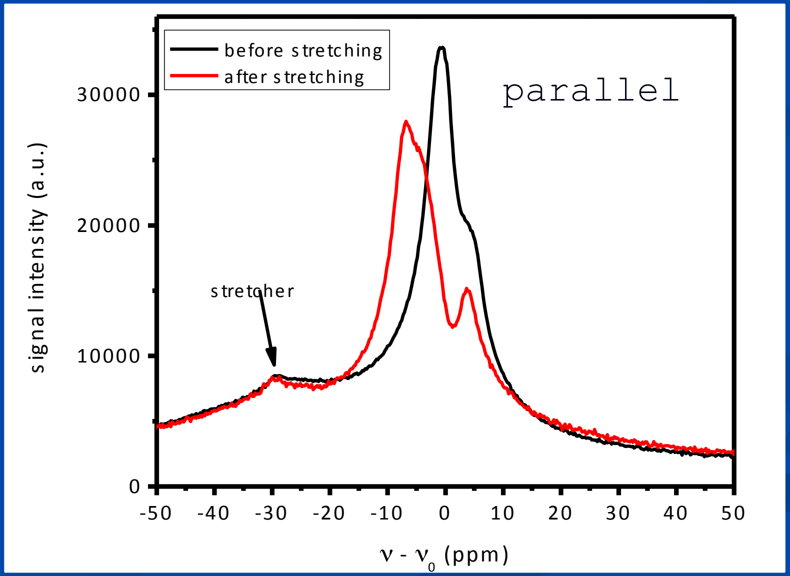

^{1}H NMR lineshapes measured by Hahn echo at υ_0 = 100 MHz of a 47 μm thick Pd foil.